JOC The Journal of Organic Chemistry

Article

pubs.acs.org/joc

Anilinomethylrhodamines: pH Sensitive Probes with Tunable Photophysical Properties by Substituent Effect

Quinn A. Best, Chuangjun Liu, Paul D. van Hoveln, Matthew E. McCarroll, and Colleen N. Scott*

Department of Chemistry & Biochemistry, Southern Illinois University, Carbondale, Illinois 62901-4409, United States

Supporting Information

ABSTRACT: A series of pH dependent rhodamine analogues possessing an anilino-methyl moiety was developed and shown to exhibit a unique photophysical response to pH. These anilinomethylrhodamines (AnMR) maintain a colorless, non-fluorescent spirocyclic structure at high pH. The spirocyclic structures open in mildly acidic conditions and are weakly fluorescent; however, at very low pH, the fluorescence is greatly enhanced. The equilibrium constants of these processes show a linear response to substituent effects, which was demonstrated by the Hammett equation.

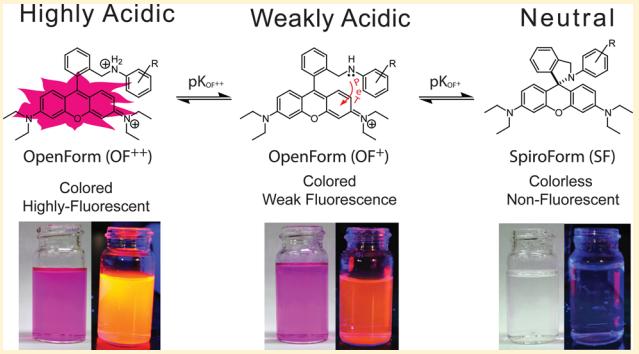

INTRODUCTION

The pH of biological systems can be diverse, ranging from slightly basic to strongly acidic. Most of these systems are known to operate under neutral or near neutral conditions; however, certain animals' and cells' organelles function under very acidic conditions. For example, lysosomes are acidic organelles where proteins and debris particles are digested under relatively acidic conditions (pH 5.5−4.5) by a variety of enzymes.[1] Abnormal deviations from these pH ranges can perturb cellular functions, which may lead to diseases. For example, abnormalities in lysosomal pH values have been linked to human breast cancer[2] and neurodegenerative disorders.[3] Another strongly acidic organ is the stomach, which contains gastric juices ranging in acidity pH from 1.5−3.0.[4] This very acidic environment activates digestive enzymes and also serves to protect the body from ingested micro-organisms by acting as a barrier for bacteria.[5] Stomach diseases can occur if the pH of the stomach in not operating at optimal conditions.[6]

Given the fundamental importance of pH in biology and the recognition of its relationship to diseases, it has become increasingly important to develop techniques to accurately measure pH with high spatiotemporal resolution for the various cellular and physiological compartments. Some of the techniques available to measure pH are positron emission topography[7] and magnetic resonance imaging (MRI);[8] however, fluorescence based techniques are one alternative to PET and MRI. Fluorescence based techniques are advantageous because of the relatively low technical costs, high sensitivity, and high spatiotemporal resolution. A variety of fluorescence-based sensors for pH have been designed over the years.[9] The main design criteria for a fluorescent pH sensor are the fluorophore's optical qualities, namely, molar absorptivity, quantum yield, and the emission and excitation wavelengths. Another important criterion is tuning the pK_a of the H^+ recognition element to the organelle or cellular pH values of interest.[9] The phenolic proton in fluorescein, and fluorescein analogues drastically influence the fluorescent properties of these molecules, which can be tuned by introducing halogen atoms to the xanthene core.[10] Carbocyanines covalently linked with amino or anilino substituents have been used to introduce a pH dependent property in the development of fluorescent pH probes.[11] However, a major drawback in the use of these fluorophores is their inherent tendency to undergo photobleaching, which is problematic for applications involving biological imaging. On the contrary, rhodamine-based fluorophores have advantages in biological imaging because of their superior photophysical properties, such as photostability and their relative ease of derivatization.

A multitude of fluorescent probes have been designed around the rhodamine spirocyclic amide scaffold,[12] which allows for a distinct "off-on" colorimetric and fluorescent response toward an intended analyte, e.g., H^+.[13] Recently, we reported an analogous rhodamine spirocyclic amine scaffold used in the optical detection of pH.[14] Since then, these aminomethylrhodamines (AMR), a.k.a. rhodamine deoxy-lactams, have also been utilized by Han et al. in the detection of nerve agents,[15] phosgene,[16] and biologically relevant aldehydes.[17] Furthermore, our work on the AMR scaffold, and more recently the work of Peterson et al.,[18] has shown that the pH range in which these probes respond can be tuned by introducing different functional groups to change the basicity of the amine moiety.

Received: July 9, 2013
Published: September 19, 2013

We are interested in exploring functionalities that can be used to tune the pH dependent properties of the AMR scaffold. We have chosen to use aniline in place of the amino group, with the goal of altering the basicity by attaching various electron withdrawing groups (EWG) or electron donating groups (EDG) substituents on the benzene ring. Herein, we report our findings on a new class of rhodamine based pH probes, which we have termed anilinomethylrhodamines (AnMR).

RESULTS AND DISCUSSION

We investigated a series of pH dependent rhodamines derived from both rhodamine B and rhodamine 6G (Figure 1). This work is a continuation of our previous work expanding on the development of optical pH probes based on rhodamine B aminomethylrhodamine (AMR). We included the rhodamine 6G fluorophore in the study because they are known to have better photophysical properties compared to rhodamine B.[19] It was also believed that the presence of the methyl groups on rhodamine 6G could influence the spirocyclic ring-opening through steric effects. Acid/base titrations were carried out and monitored by both fluorescence and UV−visible absorption techniques. The AMR and AMR6G were found to be colorless and nonfluorescent under strongly basic conditions, i.e., pH 9−12, which is attributed to the spirocyclic form (SF). However, as the solutions approach acidic pH, the characteristic colors of the AMR (λ_{abs} = 564 nm, pH = 4.6) and AMR6G (λ_{abs} = 535 nm, pH = 3.3) fluorophores become apparent, and a constant absorption maximum is maintained from pH 7−3 (Figure 2A,B). Similarly, a fluorescence enhancement is observed as the solutions of AMR (λ_{Fl} = 584 nm) and AMR6G (λ_{Fl} = 550 nm) become increasingly acidic, which correlates well with the rise in absorbance (Figure 2C,D).

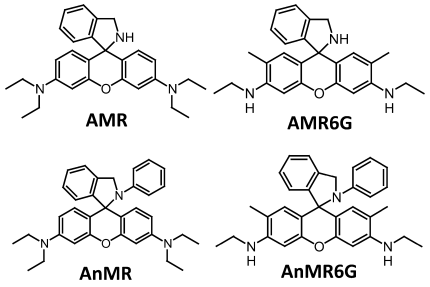

Figure 1. Structures of aminomethylrhodamines (AMR) and anilinomethylrhodamines (AnMR).

Next, we set out to investigate the effects of pH on AnMR and AnMR6G. We hypothesized that AnMR and AnMR6G would respond similarly to AMR and AMR6G, albiet at a lower pH. We synthesized AnMR and AnMR6G from the corresponding rhodamine precursors and analyzed their structures by NMR and mass spectrometry. In the ^{13}C NMR spectrum, both compounds display a quaternary carbon at a chemical shift, indicative of the spirocyclic form (see Supporting Information).

Fluorescence and UV−visible spectroscopy were also consistent with the spirocyclic form as both AnMR and AnMR6G appear colorless and nonfluorescent, which is similar to the analogous AMR based system. As expected, the anilino-analogues respond colorimetrically under more acidic conditions with respect to the corresponding AMR compounds. Figure 3A,B displays the absorption spectra for AnMR and AnMR6G, respectively. The color from AnMR becomes noticeable around pH 5 (λ_{abs} = 550 nm), whereas AnMR6G begins to respond around pH 7 (λ_{abs} = 528 nm). Like the AMR system, the absorbance of AnMR and AnMR6G increases steadily as the pH decreases; however, an unexpected red-shift in the absorption maxima occurred under very acidic conditions with little change in the actual absorption value. Interestingly, the fluorescence response of AnMR (λ_{Fl} = 591 nm, Figure 3C) and AnMR6G (λ_{Fl} = 559 nm, Figure 3D) is greatly enhanced and mirrors the red-shift observed in the absorption spectra (AnMR, Figure 3E, and AnMR6G, Figure 3F). The maximum absorbance shifts to 568 nm around pH = 3.5, and 536 nm around pH = 4 for AnMR and AnMR6G, respectively (Figure 3G,H). Initially, the low fluorescence response indicates the presence of a nonfluorescent spirocyclic form (SF) that is observed under basic conditions. Under weakly acidic conditions, solutions containing the probe become colored, albeit only weakly fluorescent. It is not until strongly acidic

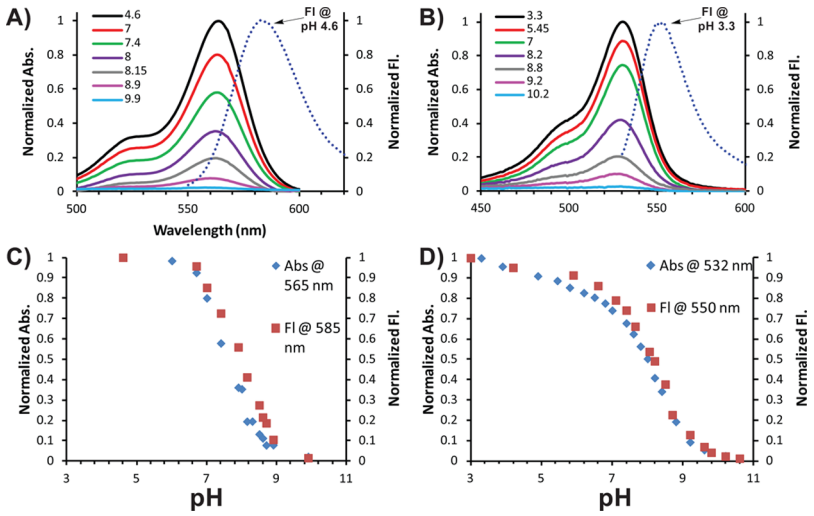

Figure 2. Spectroscopic properties of a 5 μM solution of AMR (A and C) and AMR6G (B and D) in 0.1 M sodium phosphate buffer and 0.5% DMSO at the various pH values shown. (A and B) absorbance and fluorescence with excitation at 520 and 500 nm for the AMR and AMR6G, respectively; (C and D) mapping of fluorescence and absorbance.

dx.doi.org/10.1021/jo401323g | J. Org. Chem. 2013, 78, 10134−10143

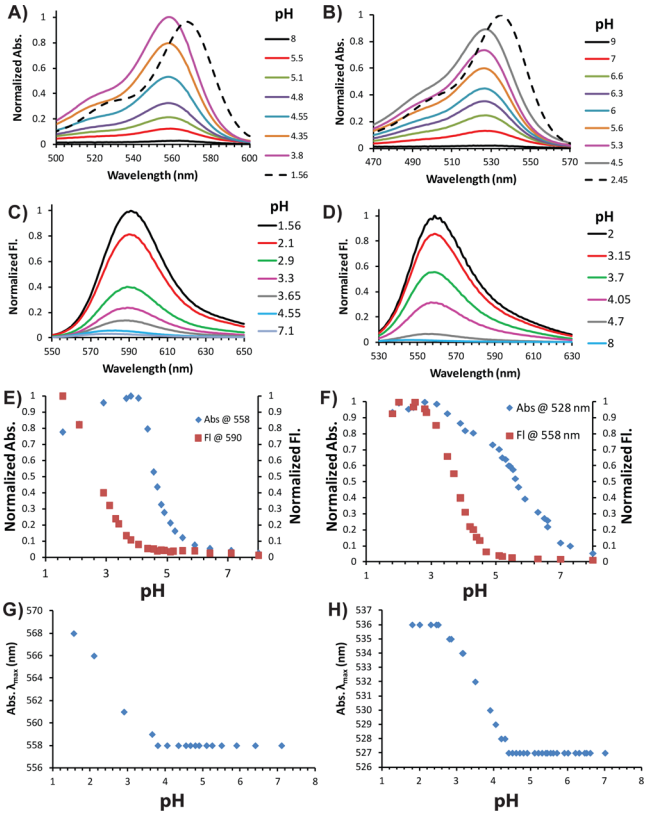

Figure 3. Spectroscopic properties of a 5 μM solution of AnMR and AnMR6G in 0.1 M sodium phosphate buffer and 0.5% DMSO at the various pH values shown. (A and B) absorbance; (C and D) fluorescence, with excitation at 520 and 500 nm for AnMR and AnMR6G, respectively; (E and F) mapping of fluorescence and absorbance; (G and H) demonstration of the shifting in the absorbance at low pH.

conditions are introduced that the probes display strong fluorescence intensity. On the basis of these results, we propose the following mechanism to describe the behavior of the AnMR system and its "unique" behavior with respect to the AMR system. Both systems maintain the spirocyclic form (SF) under basic conditions. Monoprotonation of either the amine or the aniline nitrogen facilitates ring-opening, resulting in the rhodamine cationic open form (OF^+), which can be further protonated to the dicationic open form (OF^{++}) under strong acidic conditions.

The equilibrium between the OF^+/SF can be observed as the increase in the absorption, whereas the equilibrium between the OF^{++}/OF^+ can be observed by the increase in fluorescence. In this mechanism, the weak fluorescence of the OF^+ state may be a result of partial quenching by the lone pair electrons on the anilino or amino groups via photoinduced electron transfer (PeT). In the OF^{++} state, PeT is disrupted when the lone pair electrons are now involved in bonding to the hydrogen and therefore can no longer quench the fluorophore.

Equilibrium constants for these two states (OF^+ and OF^{++}) can be approximated from the absorption and fluorescence-based titration curves. Here we define the equilibrium constant of the OF^+/SF (pK_{OF+}) process at half the change in absorbance, and for the OF^{++}/OF^+ (pK_{OF++}) process at half the change in fluorescence. From this analysis, we have estimated that the pK_{OF+} (AnMR) is 4.3, (AnMR6G) is 5.6, and the pK_{OF++} (AnMR) is 2.6 and (AnMR6G) is 3.8 (Table 1). The red-shift in the absorption spectrum highlights the change in the AnMR ground state. The AMR system does not display a red-shift, nor is there a distinct difference between the absorption or fluorescence pH titration curves, which seems to indicate that the pK_{OF+} and the pK_{OF++} are too close to be observed separetely by these techniques.

We then examined a variety of AnMR and AnMR6G compounds with variation of the subsitution on the anilino

Table 1. Spectroscopic Properties and Equilibrium Constants of the AnMR and AnMR6G Series

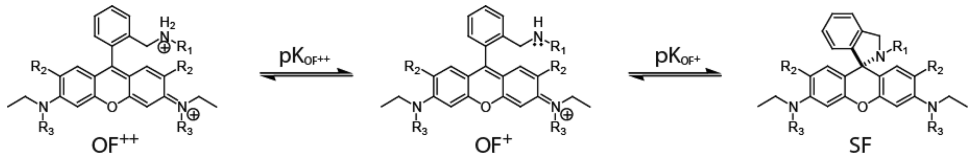

compound	λ_{abs} (nm)[a]	λ_{Fl} (nm)[a]	ε (cm^{-1} M^{-1})[a]	Fl/Fl_0[b]	pK_{OF+}	pK_{OF++}
AMR	564	584	75 000	65	8.0	7.6
AnMR	568	591	66 000	76	4.3	2.6
pMeO-AnMR	570	590	56 000	97	4.6	3.8
mMeO-AnMR	567	592	50 000	14	4.8	2.5
pMe-AnMR	570	591	67 000	78	4.0	3.4
mMe-AnMR	564	591	38 000	16	4.5	3.0
pF-AnMR	570	593	100 000	111	4.2	2.8
mF-AnMR	570	592	43 000	30	3.8	2.0
pCI-AnMR	569	591	55 000	68	3.6	2.3
mCl-AnMR	562	590	44 000	61	3.9	2.0
pCF_3-AnMR	559	588	39 000	6	3.7	–
mCF_3-AnMR	558	588	42 000	57	3.7	1.8
AMR6G	531	550	50 500	74	8.2	8.0
AnMR6G	535	559	62 000	73	5.9	3.8
pMeO-AnMR6G	536	559	46 000	85	6.9	4.0
pCI-AnMR6G	538	561	48 000	14	6.4	1.5
pCF_3-AnMR6G	551	560	64 000	79	6.0	0.8

[a]Measured in pH 1 buffer solution. [b]Measured in pH 1 buffer solution (Fl) and pH 10 buffer solution (Fl_0).

dx.doi.org/10.1021/jo401323g | J. Org. Chem. 2013, 78, 10134−10143

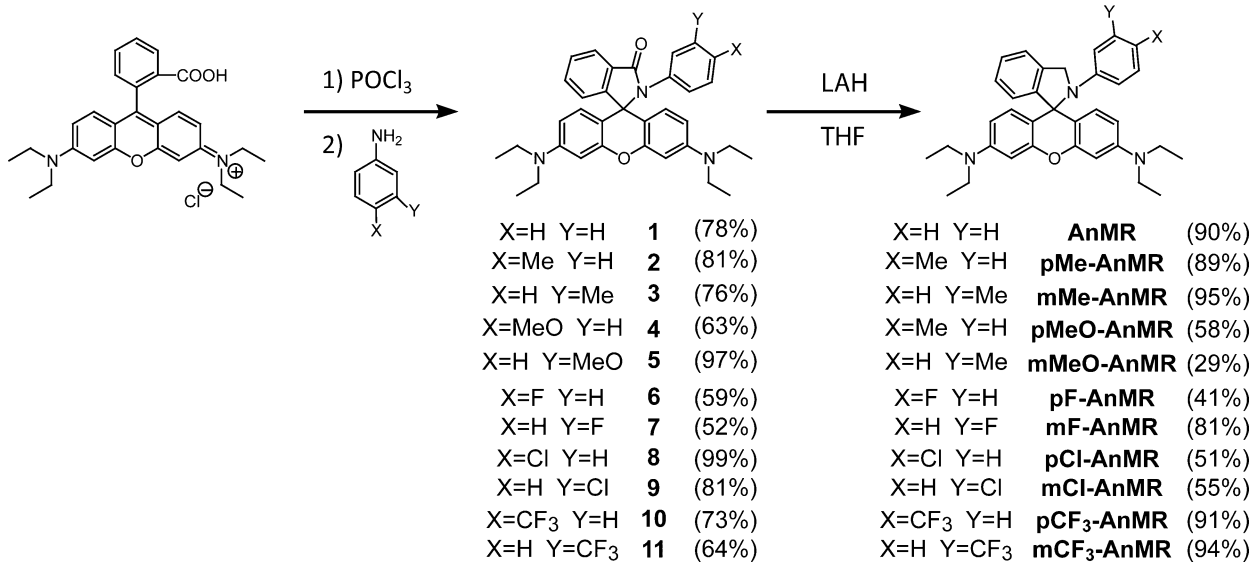

Figure 4. Synthesis of the anilinomethylrhodamine (AnMR) and their substituted analogues.

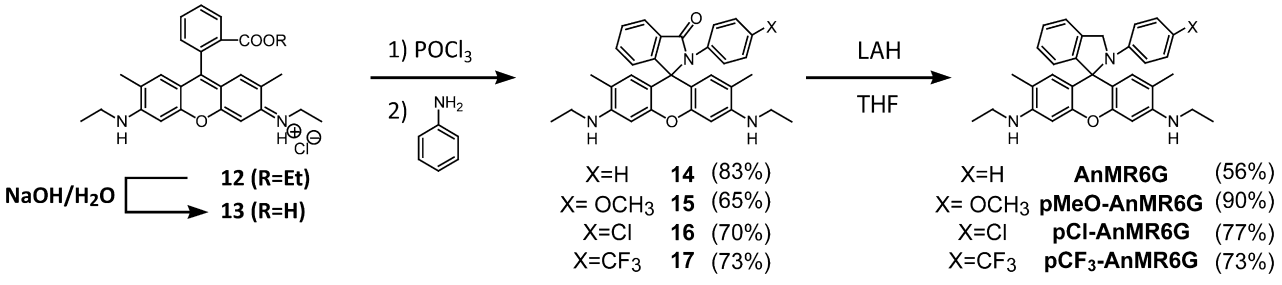

Figure 5. Synthesis of the AnMR6G series.

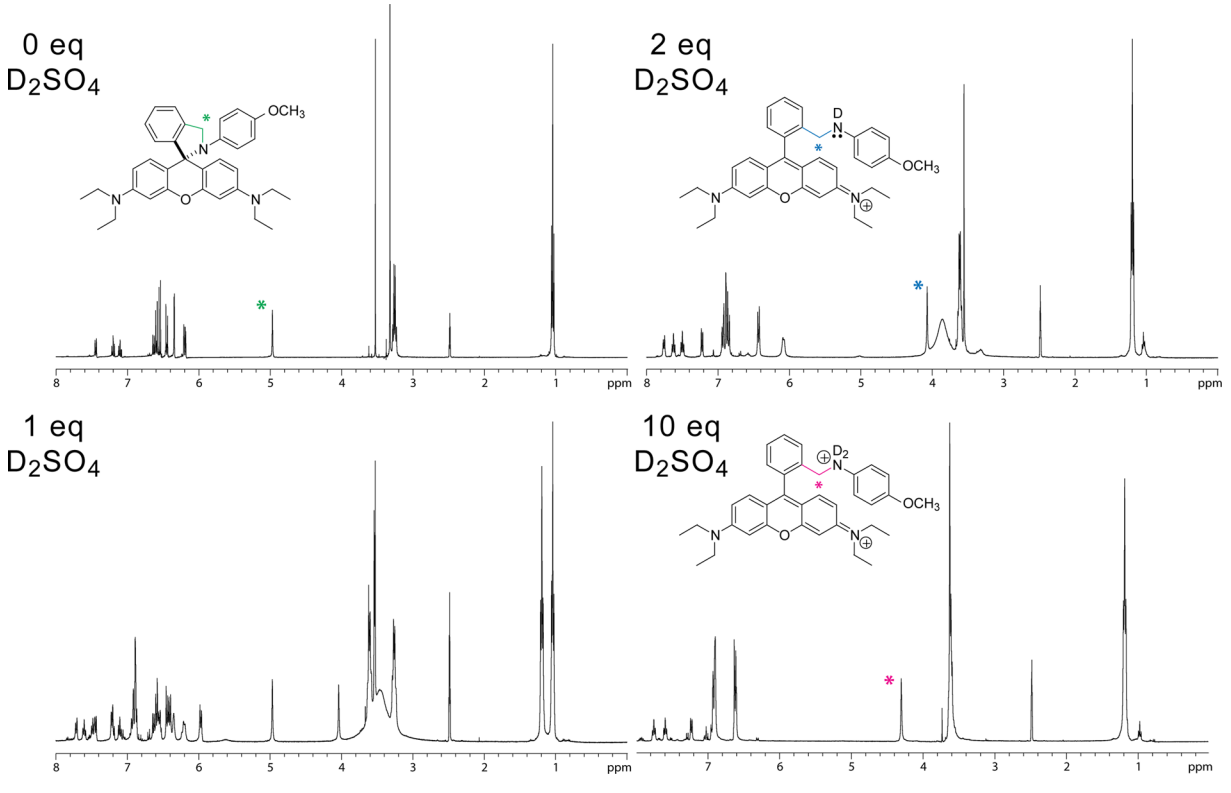

Figure 6. ^{1}H NMR titration of a 0.5 mM solution of pMeO-AnMR in DMSO-d_6 with D_2SO_4.

dx.doi.org/10.1021/jo401323g | J. Org. Chem. 2013, 78, 10134−10143

phenyl ring. These compounds were synthesized in a method similar to their AnMR and AnMR6G analogues (Figures 4 and 5) and were characterized by NMR, mass spectrometry, UV−vis, and fluorescence. All of the AnMR compounds display a similar type of behavior as their AnMR parent compound, i.e., a separate and distinct colorimetric and fluorescence response (Table 1). The low pK_a value observed for the response of these compounds (pK_{OF++} ∼ 4−1.5) suggests possible applications in very acidic regions of biological systems such as the stomach.

In general, the absorption and fluorescence for the AnMR series show a 30−40 nm red-shift compared to the AnMR6G series. There was no trend observed in the molar absorptivity data for these compounds, and the average molar absorptivity is 56 000 cm^{-1} M^{-1}. There were a few compounds that deviated from the average; noteworthy was pF-AnMR with a very high molar absorptivity of 100 000 cm^{-1} M^{-1} and mMe-AnMR and pCF_3-AnMR with low values of 38 000 and 39 000 cm^{-1} M^{-1}, respectively (Table 1). The limited number of compounds in the AnMR6G series hinders the formation of a definite conclusion; however, one compound, pCF_3-AnMR6G (64 000 cm^{-1} M^{-1}), stands out as having a higher molar absorptivity than the others. There was no noticeable trend for the fluorescence enhancement (Fl/Fl_o) for either series. However, some compounds show very low fluorescence enhancement among the AnMR and AnMR6G series. Among the AnMR series, pCF_3-AnMR showed a remarkably low fluorescence enhancement of 6, while mMeO-AnMR and mMe-AnMR also showed a small fluorescence enhancement of 14 and 16, respectively. In the AnMR6G series, one low fluorescence enhancement was observed in pCl-AnMR6G with a fluorescence enhancement of 14. The precise nature of the lower fluorescence enhancement observed by these species remains unknown, but presumably some quenching by the substituents themselves may be occurring. The quantum yield was measured for two representative compounds from each series to compare the two probe systems. Acidic conditions (pH 1.5), where a maximum amount of fluorescence was observed, were invoked when measuring pMeO-AnMR and pMeO-AnMR6G, which had quantum yields of 14 and 65%, respectively, using rhodamine B in ethanol (Φ = 0.49)[20] as a standard (see Supporting Information).

Although the fluorescence and UV−vis data provide strong evidence for the proposed mechanism, we carried out NMR experiments on an AnMR derivative to elucidate the structural changes occurring under similar conditions. A solution of pMeO-AnMR was prepared in DMSO-d_6 and titrated with aliquots of D_2SO_4 while changes in the structure were monitored by NMR (Figure 6). New signals in the NMR spectrum corresponding to a drastic change in the pMeO-AnMR structure were observed upon adding D_2SO_4. The benzylic protons gave the clearest signal and was ultimately used in determing the stuctural changes that were occurring.

In the absence of D_2SO_4, pMeO-AnMR maintains the SF with a benzylic signal at 4.98 ppm. The addition of 1 equiv of D_2SO_4 creates a new set of signals, notably a new signal at 4.05 ppm and a reduction in the 4.98 ppm signal intensity. By 2 equiv of D_2SO_4, there is no longer a signal at 4.98 ppm, nor is there anymore increase in the signal intensity at 4.05, which is believed to be a new strucuture. The generation of the distinctly new and unique proton signals in the NMR structure is indicative of the molecule reacting and undergoing a major change in the structure when D_2SO_4 is added. Interestingly, further changes in the NMR spectrum occur as additions of D_2SO_4 leading to 10 equiv causes downfield shift in the benzylic signal from 4.05 ppm to 4.35 ppm and is thought to occur from the formation of the anilinium cation or the OF^{++}. A comparison to the AMR series was made (see Supporting Information), where similar changes between the SF and OF^+ were observed; however, there was no further shifting of the benzylic signal with increasing equivalents of D_2SO_4 indicating that the ammonium cation is quickly formed and there is no distinction between the OF^+ and OF^{++}. From the NMR, the distinct structural changes between the SF to OF^+ and the OF^+ to OF^{++} can be distinguished by either the formation of new ^1H NMR signals or from the shift in the benzylic ^1H NMR signal. These results corroborate the differences in the AnMR and AMR mechanism observed by fluorescence and UV−vis.

As predicted, the acid/base properties of the AnMR system were affected by the presence of EDG or EWG. From the UV−vis and fluorescence titrations curves, the pK_{OF+} and the pK_{OF++} were estimated for each compound (see Supporting Information). The effects of the substituents on the equilibrium constants of the reaction can be predicted by the Hammett equation. The pK_{OF+} and pK_{OF++} for each AnMR and AnMR6G compound were plotted against their respective Hammett σ constants and compared with published experimental data from similar aniline derivatives.[21] We were pleased to find that the overall trend of the pK_{OF+} and the pK_{OF++} for AnMR analogues follows typical Hammet-like behavior, i.e., a negative slope in the pK_a with respect to the corresponding σ constants (Figure 7). The R^2 values for the AnMR OF^{++} and the AnMR6G OF^{++}

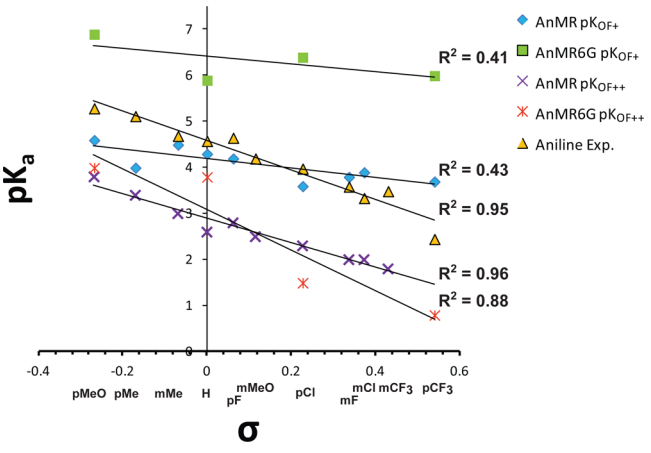

Figure 7. A comparison of the Hammett plots for the pK_{OF+} and pK_{OF++} of the AnMR and AnMR6G series and aniline.

both had comaparable fit to that of the literature aniline series, although there are some anomal values for the AnMR6G OF^{++} series. The AnMR OF^+ and AnMR6G OF^+ gave poor R^2 values, perhaps due to deviation of a few data points from the mean. It is evident from these plots, however, that the equilibrium between the spirocyclic ring (SF) and the open form (OF^+), and the (OF^+) and (OF^{++}) structures was being influenced substantially by the substituents on the aniline ring and thus produces difference in the pK_a for the protonated (pK_{OF+}) and diprotonated (pK_{OF++}) anilines.

CONCLUSION

In conclusion, a series of novel fluorescent probes for the optical measurement of acidic pH has been developed based on

dx.doi.org/10.1021/jo401323g | J. Org. Chem. 2013, 78, 10134−10143

the AnMR system. These probes display distinct and separate colorimetric and fluorescent responses at different pH values. We propose that the differences in the colorimetric and fluorescence response can be explained by an initial opening of the spirocycle form (SF) upon protonation in weakly acidic conditions, resulting in the weakly fluorescent monocationic open form (OF^+). Further protonation under increasingly acidic conditions results in the highly fluorescent dication open form (OF^{++}). The equilibrium constants for these reactions, OF^+/SF and OF^{++}/OF^+, can be measured by UV−vis absorption and fluorescence, respectively. The results of NMR based studies corroborate the proposed mechanism. The equilibrium constants display a linear relationship when plotted against the Hammett σ constants for the AnMR OF^{++} and AnMR6G OF^{++} series based on the R^2 values; however, the linear plot for the AnMR OF^+ and AnMR6G OF^+ series did not fit as well. More data points will be developed to establish a more accurate relationship for all the series. We will probe the nature of the low fluorescence enhancement in some of the substituted AnMR and AnMR6G series. Biological studies utilizing AnMR as a probe for measuring intracellular pH are ongoing.

EXPERIMENTAL SECTION

General chemicals were purchased from commercial sources and used without further purification unless otherwise stated. DMF, acetone, methylene chloride, chloroform and ethyl acetate were all reagent grade and used without further purification unless otherwise mentioned. THF was obtained from solvent purification system. Analytical thin layer chromatography (TLC) was conducted on precoated TLC plates, silica gel 60 F254, layer thickness 0.25 mm. Column chromatography was performed on an isolera 4 with an ultraviolet detector.

^{1}H NMR, ^{13}C NMR, DEPT, and NOESY spectra were recorded on a 400 or 300 MHz instrument using deuterated chloroform ($CDCl_3$), methanol (CD_3OD) and dimethyl sulfoxide [$(CD_3)_2SO$]. Chemical shifts are reported in delta (δ) parts per million (ppm). Splitting patterns are abbreviated as follows: s, singlet; d, doublet; t, triplet; q, quartet; m, multiplet; br, broad.

Mass spectra (MS) were measured on a GC−MS, a Quattro II, or a Q-TOF Ultima. Absorbance data were obtained using a UV−vis spectrometer. Fluorescence spectra were recorded on a modular spectrofluorometer.

pH Titrations. The following procedure was used for the spectroscopic analysis of the AnMR pH probes. In a 200 mL beaker, 50 mL of either a 2.5 μM (fluorescence) or a 5 μM (UV−vis) solution of the corresponding sensor in 0.1 M sodium phosphate buffer and 0.5% DMSO was allowed to stir in open air for approximately 0.5 h, allowing the solution to become saturated with oxygen. AnMR6G solutions were similarly prepared, with the exception that a 2.5 μM concentration was used for both fluorescence and UV−vis. Using a digital pH meter equipped with a glass electrode (pH/ATC calomel) the pH was monitored and adjusted to acidic or basic conditions using small aliquots of conc. HCl or a 4.0 M NaOH solution, respectively. The pH was allowed to stabilize for ∼1 min, and then 3.0 mL of the solution was added to a quartz cuvette for analysis. The spectra are found in the Supporting Information.

Synthesis of Compounds 1−11. A general procedure for preparing the rhodamine B amides (**1**−**11**) was used. To a solution of rhodamine B (400 mg, 0.84 mmol) in 1,2-dichloroethane (10 mL) was added phosphorus oxychloride (0.3 mL, 3 mmol) dropwise. The solution was refluxed for 4 h. The reaction mixture was cooled and concentrated under reduced pressure to give the rhodamine B acid chloride, which was used in the next step without further purification. The crude acid chloride was dissolved in 1,2-dichloroethane (10 mL), and to the solution was added 0.15 mL of the corresponding aniline. This solution was allowed to stir for 24 h, which was then transferred to a separatory funnel with an additional 20 mL of dichloromethane (DCM). The organic layer was washed with 2.0 M H_2SO_4 solution (3 × 20 mL) and then with water (2 × 20 mL), and finally 0.10 M solution (2 × 20 mL). The organic layer was then dried over anhydrous $MgSO_4$ and evaporated in vacuo. The products were purified by column chromatography on alumina (neutral) with 70:30 hexanes:EtOAc.

*3′,6′-Bis(diethylamino)-2-phenyl-2,3-dihydrospiro[isoindole-1,9′-xanthene]-3-one (**1**).* Previously synthesized.[22] Yield 368 mg (85%): R_f = 0.4 in 70:30 Hex:EtOAc; ^{1}H NMR (400 MHz, $CDCl_3$) δ 8.00 (dd, J = 4.6, 2.4 Hz, 1H), 7.59−7.42 (m, 2H), 7.21−6.94 (m, 4H), 6.79 (dd, J = 8.0, 1.8 Hz, 2H), 6.63 (d, J = 8.8 Hz, 2H), 6.30 (dd, J = 8.8, 2.6 Hz, 2H), 6.25 (s, 2H), 3.31 (q, J = 7.2 Hz, 8H), 1.14 (t, J = 7.0 Hz, 12H); ^{13}C NMR (101 MHz, $CDCl_3$) δ 167.7, 153.3, 153.1, 152.6, 148.7, 136.7, 132.8, 131.0, 128.8, 128.5, 128.1, 127.3, 126.7, 124.0, 123.3, 108.2, 108.1, 106.4, 106.0, 105.0, 97.8, 91.6, 67.5, 44.5, 44.3, 12.6.

*3′,6′-Bis(diethylamino)-2-(4-methylphenyl)-2,3-dihydrospiro-[isoindole-1,9′-xanthene]-3-one (**2**).* Pink amorphous solid. Yield 360 mg (81%): R_f = 0.38 in 70:30 Hex:EtOAc; ^{1}H NMR (400 MHz, $CDCl_3$) δ 8.02 (dd, J = 7.0, 2.2 Hz, 1H), 7.59−7.40 (m, 2H), 7.15 (dd, J = 7.0, 2.2 Hz, 1H), 6.90 (d, J = 7.9 Hz, 2 H), 6.64 (m, 4H), 6.31 (dd, J = 8.9, 2.6 Hz, 2H), 6.25 (d, J = 2.6 Hz, 2H), 3.31 (q, J = 7.2 Hz, 8H), 2.20 (s, 3H), 1.15 (t, J = 7.1 Hz, 12H); ^{13}C NMR (101 MHz, $CDCl_3$) δ 168.2, 167.7, 153.1, 153.18, 153.17, 151.9, 149.4, 148.7, 136.3, 133.8, 132.7, 131.2, 129.27, 129.25, 129.24, 128.9, 128.12, 128.05, 127.32, 127.27, 124.0, 123.3, 110.0, 108.2, 108.1, 106.5, 97.8, 67.3, 44.5, 44.3, 27.0, 21.08, 21.06, 14.7, 12.6; HRMS (ESI-TOF) m/z [M + H]$^+$ Calcd for $C_{35}H_{37}N_3O_2$ 532.2964, found 532.2955.

*3′,6′-Bis(diethylamino)-2-(3-methylphenyl)-2,3-dihydrospiro-[isoindole-1,9′-xanthene]-3-one (**3**).* Pink amorphous solid. Yield 338 mg (76%): R_f = 0.38 in 70:30 Hex:EtOAc; ^{1}H NMR (400 MHz, $CDCl_3$) δ 8.05−7.90 (m, 1H), 7.54−7.43 (m, 2H), 7.21−7.14 (m, 1H), 6.98 (t, J = 7.7 Hz, 1H), 6.90 (d, J = 7.6 Hz, 1H), 6.63 (d, J = 8.8 Hz, 2H), 6.57 (d, J = 2.0 Hz, 1H), 6.49 (d, J = 7.8 Hz 1H), 6.32 (dd, J = 8.8, 2.6 Hz, 2H), 6.24 (d, J = 2.6 Hz, 2H), 3.32 (q, J = 7.2 Hz, 8H), 2.11 (s, 3H), 1.14 (t, J = 7.0 Hz, 12H); ^{13}C NMR (101 MHz, $CDCl_3$) δ 167.5, 153.2, 153.1, 151.0, 149.4, 148.7, 146.0, 138.0, 136.4, 132.7, 131.4, 128.9, 128.5, 128.2, 128.1, 127.64, 127.60, 124.32, 124.26, 124.0, 123.3, 108.2, 108.1, 106.6, 97.8, 91.4, 69.2, 67.5, 44.4, 38.3, 21.3, 14.7, 12.6; HRMS (ESI-TOF) m/z [M + H]$^+$ Calcd for $C_{35}H_{37}N_3O_2$ 532.2964, found 532.2964.

*3′,6′-Bis(diethylamino)-2-(4-methoxyphenyl)-2,3-dihydrospiro-[isoindole-1,9′-xanthene]-3-one (**4**).* Pink amorphous solid. Yield 289 mg (63%): R_f = 0.28 in 70:30 Hex:EtOAc; ^{1}H NMR (400 MHz, $CDCl_3$) δ 8.06−7.95 (m, 1H), 7.56−7.44 (m, 2H), 7.17 (dd, J = 5.3, 3.3 Hz, 1H), 6.71−6.53 (m, 6H), 6.42−6.17 (m, 4H), 3.68 (s, 3H), 3.32 (dd, J = 15.1, 8.0 Hz, 8H), 1.15 (t, J = 7.0 Hz, 12H); ^{13}C NMR (101 MHz, $CDCl_3$) δ 167.6, 158.2, 153.2, 148.7, 132.6, 131.4, 129.01, 128.95, 128.1, 124.0, 123.3, 113.9, 108.1, 97.8, 67.3, 55.2, 44.4, 12.5; HRMS (ESI-TOF) m/z [M + H]$^+$ Calcd for $C_{35}H_{38}N_3O_3$ 548.2913, found 548.2915.

*3′,6′-Bis(diethylamino)-2-(3-methoxyphenyl)-2,3-dihydrospiro-[isoindole-1,9′-xanthene]-3-one (**5**).* Pink amorphous solid. Yield 446 mg (97%): R_f = 0.31 in 70:30 Hex:EtOAc; ^{1}H NMR (400 MHz, $CDCl_3$) δ 8.08−7.96 (m, 1H), 7.57−7.43 (m, 2H), 7.22−7.12 (m, 1H), 7.01 (t, J = 8.1 Hz, 1H), 6.64 (d, J = 8.7 Hz, 3H), 6.46 (d, J = 7.9 Hz, 1H), 6.39−6.21 (m, 5H), 3.48 (s, 3H), 3.31 (q, J = 6.8 Hz, 8H), 1.14 (t, J = 7.0 Hz, 12H); ^{13}C NMR (101 MHz, $CDCl_3$) δ 167.4, 159.3, 153.2, 153.0, 148.7, 137.6, 132.8, 131.2, 129.0, 128.9, 128.1, 124.0, 123.7, 119.8, 114.0, 111.4, 108.0, 106.4, 97.7, 67.5, 54.8, 44.3, 12.5; HRMS (ESI-TOF) m/z [M + H]$^+$ Calcd for $C_{35}H_{38}N_3O_3$ 548.2913, found 548.2905.

*3′,6′-Bis(diethylamino)-2-(4-fluorophenyl)-2,3-dihydrospiro-[isoindole-1,9′-xanthene]-3-one (**6**).* Pink amorphous solid. Yield 265 mg (59%): R_f = 0.41 in 70:30 Hex:EtOAc; ^{1}H NMR (400 MHz, $CDCl_3$) δ 8.01 (dd, J = 7.1, 1.6 Hz, 1H), 7.51 (dd, J = 3.8, 3.2 Hz, 2H), 7.18 (dd, J = 7.1, 1.4 Hz, 1H), 6.81 (t, J = 8.5 Hz, 2H), 6.69 (dd, J = 8.5, 5.1 Hz, 2H), 6.65−6.57 (m, 2H), 6.32 (dd, J = 8.8, 2.1 Hz, 2H), 6.25 (d, J = 2.2 Hz, 2H), 3.42−3.20 (m, 8H), 1.15 (t, J = 7.0 Hz,

dx.doi.org/10.1021/jo401323g | J. Org. Chem. 2013, 78, 10134−10143

12H); ^{13}C NMR (101 MHz, $CDCl_3$) δ 167.6, 162.5, 160.1, 153.2, 152.9, 148.8, 132.8, 132.41, 132.38, 131.1, 129.4, 129.3, 128.8, 128.2, 124.1, 123.4, 115.6, 115.3, 108.1, 106.1, 97.7, 67.5, 44.3, 12.6; HRMS (ESI-TOF) m/z [M + H]$^+$ Calcd for $C_{34}H_{35}N_3O_2F$ 536.2713, found 536.2718.

*3′,6′-Bis(diethylamino)-2-(3-fluorophenyl)-2,3-dihydrospiro-[isoindole-1,9′-xanthene]-3-one (**7**).* Pink amorphous solid. Yield 234 mg (52%): R_f = 0.45 in 70:30 Hex:EtOAc; ^{1}H NMR (400 MHz, $CDCl_3$) δ 8.04−7.97 (m, 1H), 7.56−7.45 (m, 2H), 7.17−7.12 (m, 1H), 7.12−7.03 (m, 1H), 6.83−6.73 (m, 1H), 6.73−6.65 (m, 2H), 6.64−6.58 (m, 2H), 6.31 (d, J = 2.6 Hz, 1H), 6.29 (d, J = 1.5 Hz, 3H), 3.32 (qd, J = 7.1, 1.4 Hz, 8H), 1.15 (t, J = 7.1 Hz, 12H); ^{13}C NMR (101 MHz, $CDCl_3$) δ 167.7, 163.6, 161.1, 153.4, 153.0, 148.8, 138.5, 138.4, 133.1, 130.3, 129.4, 129.3, 128.6, 128.2, 123.9, 123.4, 122.2, 122.1, 114.0, 113.8, 113.4, 113.2, 108.2, 106.1, 97.8, 67.5, 44.3, 12.6; HRMS (ESI-TOF) m/z [M + H]$^+$ Calcd for $C_{34}H_{35}N_3O_2F$ 536.2713, found 536.2707.

*3′,6′-Bis(diethylamino)-2-(4-chlorophenyl)-2,3-dihydrospiro-[isoindole-1,9′-xanthene]-3-one (**8**).* Pink amorphous solid. Yield 459 mg (99%): R_f = 0.48 in 70:30 Hex:EtOAc; ^{1}H NMR (400 MHz, $CDCl_3$) δ 8.01 (d, J = 6.2 Hz, 1H), 7.58−7.41 (m, 2H), 7.20−7.13 (m, 1H), 7.09 (d, J = 8.8 Hz, 2H), 6.78 (d, J = 8.8 Hz, 2H), 6.61 (d, J = 8.8 Hz, 2H), 6.36−6.24 (m, 4H), 3.33 (q, J = 7.3 Hz, 8H), 1.16 (t, J = 7.0 Hz, 12H); ^{13}C NMR (101 MHz, $CDCl_3$) δ 167.7, 153.2, 153.1, 148.8, 135.3, 133.0, 132.1, 130.6, 128.74, 128.68, 128.3, 128.2, 124.0, 123.4, 108.2, 106.0, 97.8, 67.5, 44.3, 12.6; HRMS (ESI-TOF) m/z [M + H]$^+$ Calcd for $C_{34}H_{35}N_3O_2Cl$ 552.2418, found 552.2418.

*3′,6′-Bis(diethylamino)-2-(3-chlorophenyl)-2,3-dihydrospiro-[isoindole-1,9′-xanthene]-3-one (**9**).* Pink amorphous solid. Yield 375 mg (81%): R_f = 0.48 in 70:30 Hex:EtOAc; ^{1}H NMR (400 MHz, $CDCl_3$) δ 8.00 (d, J = 6.4 Hz, 1H), 7.59−7.43 (m, 2H), 7.16 (d, J = 6.3 Hz, 1H), 7.09−6.97 (m, 2H), 6.90 (s, 1H), 6.68 (d, J = 7.5 Hz, 1H), 6.60 (d, J = 8.7 Hz, 2H), 6.38−6.25 (m, 4H), 3.32 (q, J = 7.4 Hz, 8H), 1.15 (t, J = 7.0 Hz, 12H); ^{13}C NMR (101 MHz, $CDCl_3$) δ 167.5, 153.1, 148.9, 138.0, 133.8, 133.1, 130.6, 129.4, 128.4, 128.2, 127.3, 126.6, 124.8, 124.0, 123.4, 108.3, 106.1, 97.9, 67.6, 44.4, 12.6; HRMS (ESI-TOF) m/z [M + H]$^+$ Calcd for $C_{34}H_{35}N_3O_2Cl$ 552.2418, found 552.2415.

*3′,6′-Bis(diethylamino)-2-[4-(trifluoromethyl)phenyl]-2,3-dihydrospiro[isoindole-1,9′-xanthene]-3-one (**10**).* Pink amorphous solid. Yield 357 mg (73%): R_f = 0.65 in 80:20 Hex:EtOAc; ^{1}H NMR (400 MHz, $CDCl_3$) δ 7.99 (d, J = 1.9 Hz, 1H), 7.60−7.44 (m, 2H), 7.39 (d, J = 8.5 Hz, 2H), 7.16−7.04 (m, 3H), 6.61 (d, J = 9.0 Hz, 2H), 6.29 (m, 4H), 3.32 (q, J = 7.2 Hz, 8H), 1.15 (t, J = 7.0 Hz, 12H); ^{13}C NMR (101 MHz, $CDCl_3$) δ 168.3, 153.4, 152.9, 148.8, 140.0, 133.4, 129.8, 128.40, 128.35, 126.4, 125.63, 125.59, 125.55, 124.0, 123.3, 108.2, 105.5, 97.8, 67.9, 44.2, 12.4; HRMS (ESI-TOF) m/z [M + H]$^+$ Calcd for $C_{35}H_{35}N_3O_2F_3$ 586.2681, found 586.2675.

*3′,6′-Bis(diethylamino)-2-[3-(trifluoromethyl)phenyl]-2,3-dihydrospiro[isoindole-1,9′-xanthene]-3-one (**11**).* Pink amorphous solid. Yield 313 mg (64%): R_f = 0.56 in 70:30 Hex:EtOAc; ^{1}H NMR (400 MHz, $CDCl_3$) δ 8.02 (dd, J = 6.0, 2.1 Hz, 1H), 7.57−7.48 (m, 2H), 7.34 (d, J = 7.9 Hz, 1H), 7.25−7.18 (m, 2H), 7.03−6.93 (m, 2H), 6.61 (d, J = 8.7 Hz, 2H), 6.32 (dd, J = 8.9, 2.6 Hz, 2H), 6.24 (d, J = 2.6 Hz, 2H), 3.31 (q, J = 7.1 Hz, 8H), 1.14 (t, J = 7.0 Hz, 12H); ^{13}C NMR (101 MHz, $CDCl_3$) δ168.3, 153.4, 152.9, 148.9, 140.0, 133.4, 129.8, 128.4, 128.0 (q, J^2 = 32.5 Hz) 126.4, 125.6 (q, J^3 = 3.7 Hz), 124.0, 123.9 (q, J^1 = 272 Hz) 123.3, 108.2, 105.5, 97.8, 67.8, 44.4, 12.4; HRMS (ESI-TOF) m/z [M + H]$^+$ Calcd for $C_{35}H_{35}N_3O_2F_3$ 586.2681, found 586.2697.

Synthesis of the Anilinomethylrhodamine (AnMR) and Their Substituted Analogues. A general procedure for AnMR, pMe-AnMR, mMe-AnMR, pMeO-AnMR, mMeO-AnMR, pF-AnMR, mF-AnMR, pCl-AnMR, mCl-AnMR, pCF$_3$-AnMR, and mCF$_3$-AnMR was used. In a 50 mL round-bottom flask, 100 mg of the rhodamine amide was dissolved in 30 mL of dry THF. To this solution, 80 mg of $LiAlH_4$ was slowly added, and the mixture was stirred at room temperature for 12 h. The reaction was quenched by slowly adding 0.5 mL of water, followed by 1 mL of 15% NaOH. The mixture was filtered and the filtrate dried using $MgSO_4$. The THF was removed under reduced pressure. The products were purified by column chromatography on alumina (neutral) with 90:10 hexanes:EtOAc.

3′-N,3′-N,6′-N,6′-N-Tetraethyl-2-phenyl-2,3-dihydrospiro-[isoindole-1,9′-xanthene]-3′,6′-diamine (AnMR). Pink viscous oil. Yield 70 mg (72%): R_f = 0.5 in 90:10 Hex:EtOAc; ^{1}H NMR (400 MHz, $CDCl_3$) δ 7.39 (d, J = 7.6 Hz, 1H), 7.20 (t, J = 7.4 Hz, 1H), 7.12 (t, J = 7.5 Hz, 1H), 7.05 (t, J = 7.7 Hz, 2H), 6.88 (d, J = 7.7 Hz, 1H), 6.65 (m, 4H), 6.57 (t, J = 7.2 Hz, 1H), 6.42 (d, J = 2.5 Hz, 2H), 6.19 (dd, J = 8.8, 2.5 Hz, 2H), 5.06 (s, 2H), 3.29 (q, J = 7.1 Hz, 8H), 1.13 (t, J = 7.0 Hz, 12H); ^{13}C NMR (101 MHz, $CDCl_3$) δ 188.2, 174.7, 167.4, 151.9, 151.1, 148.1, 144.4, 143.2, 132.6, 128.54, 128.48, 128.0, 126.7, 124.0, 121.8, 115.8, 113.5, 113.2, 108.1, 105.0, 97.9, 67.4, 55.0, 44.2, 29.4, 12.7; HRMS (ESI-TOF) m/z [M + H]$^+$ Calcd for $C_{34}H_{38}N_3O$ 504.3015, found 504.3019.

3′-N,3′-N,6′-N,6′-N-Tetraethyl-2-(4-methylphenyl)-2,3-dihydrospiro[isoindole-1,9′-xanthene]-3′,6′-diamine (pMe-AnMR). Pink viscous oil. Yield 87 mg (89%): R_f = 0.55 in 90:10 Hex:EtOAc; ^{1}H NMR (400 MHz, $CDCl_3$) δ 7.37 (d, J = 7.5 Hz, 1H), 7.19 (t, J = 7.4 Hz, 1H), 7.11 (t, J = 7.5 Hz, 1H), 6.86 (m, 3H), 6.65 (d, J = 8.6 Hz, 2H), 6.55 (d, J = 8.6 Hz, 2H), 6.41 (d, J = 2.5 Hz, 2H), 6.18 (dd, J = 8.8, 2.6 Hz, 2H), 5.04 (s, 2H), 3.29 (q, J = 7.0 Hz, 8H), 2.13 (s, 3H), 1.13 (t, J = 7.0 Hz, 12H); ^{13}C NMR (101 MHz, $CDCl_3$) δ 151.9, 151.2, 148.1, 142.2, 132.9, 129.2, 128.5, 128.0, 126.7, 124.6, 124.0, 121.9, 113.5, 113.4, 108.1, 97.9, 67.3, 55.1, 44.3, 20.5, 12.8, 12.7; HRMS (ESI-TOF) m/z [M + H]$^+$ Calcd for $C_{35}H_{40}N_3O$ 518.3171, found 518.3170.

3′-N,3′-N,6′-N,6′-N-Tetraethyl-2-(3-methylphenyl)-2,3-dihydrospiro[isoindole-1,9′-xanthene]-3′,6′-diamine (mMe-AnMR). Pink viscous oil. Yield 92 mg (95%): R_f = 0.55 in 90:10 Hex:EtOAc; ^{1}H NMR (400 MHz, $CDCl_3$) δ 7.38 (d, J = 7.5 Hz, 1H), 7.20 (t, J = 7.3 Hz, 1H), 7.12 (t, J = 7.4 Hz, 1H), 6.93−6.81 (m, 2H), 6.65 (d, J = 8.7 Hz, 2H), 6.53 (t, J = 1.9 Hz, 1H), 6.46−6.32 (m, 4H), 6.19 (dd, J = 8.8, 2.6 Hz, 2H), 5.05 (s, 2H), 3.29 (q, J = 7.1 Hz, 8H), 2.22 (s, 3H), 1.13 (t, J = 7.0 Hz, 12H); ^{13}C NMR (101 MHz, $CDCl_3$) δ 151.9, 151.2, 148.1, 144.4, 138.1, 132.8, 128.6, 128.3, 128.0, 126.7, 124.1, 121.8, 116.8, 114.0, 113.4, 111.1, 108.2, 97.9, 67.4, 55.1, 44.3, 22.0, 12.7; HRMS (ESI-TOF) m/z [M + H]$^+$ Calcd for $C_{35}H_{40}N_3O$ 518.3171, found 518.3173.

3′-N,3′-N,6′-N,6′-N-Tetraethyl-2-(4-methoxyphenyl)-2,3-dihydrospiro[isoindole-1,9′-xanthene]-3′,6′-diamine (pMeO-AnMR). Pink viscous oil. Yield 55 mg (56%): R_f = 0.42 in 90:10 Hex:EtOAc; ^{1}H NMR (400 MHz, $CDCl_3$) δ 7.39 (d, J = 7.5 Hz, 1H), 7.20 (t, J = 7.4 Hz, 1H), 7.12 (t, J = 7.5 Hz, 1H), 6.88 (d, J = 7.6 Hz, 1H), 6.67 (d, J = 9.2 Hz, 4H), 6.58 (d, J = 9.1 Hz, 2H), 6.43 (s, 2H), 6.21 (d, J = 8.8 Hz, 2H), 5.04 (s, 2H), 3.66 (s, 3H), 3.30 (q, J = 7.0 Hz, 8H), 1.14 (t, J = 7.5 Hz, 12H); ^{13}C NMR (101 MHz, $CDCl_3$) δ 152.0, 151.3, 150.7, 148.1, 139.0, 133.1, 128.6, 128.0, 126.7, 124.1, 121.9, 114.4, 114.1, 113.6, 108.1, 98.0, 67.4, 55.6, 55.3, 44.3, 12.8; HRMS (ESI-TOF) m/z [M + H]$^+$ Calcd for $C_{35}H_{40}N_3O_2$ 534.3121, found 534.3116.

3′-N,3′-N,6′-N,6′-N-Tetraethyl-2-(3-methoxyphenyl)-2,3-dihydrospiro[isoindole-1,9′-xanthene]-3′,6′-diamine (mMeO-AnMR). Pink viscous oil. Yield 28 mg (29%): R_f = 0.42 in 90:10 Hex:EtOAc; ^{1}H NMR (400 MHz, $CDCl_3$) δ 7.39 (d, J = 7.6 Hz, 1H), 7.21 (t, J = 7.0 Hz, 1H), 7.13 (t, J = 7.4 Hz, 1H), 6.95 (t, J = 8.2 Hz, 1H), 6.86 (d, J = 7.7 Hz, 1H), 6.64 (d, J = 8.8 Hz, 2H), 6.38 (d, J = 2.6 Hz, 2H), 6.27−6.11 (m, 5H), 5.02 (s, 2H), 3.57 (s, 3H), 3.29 (q, J = 7.1 Hz, 8H), 1.13 (t, J = 7.0 Hz, 12H); ^{13}C NMR (101 MHz, $CDCl_3$) δ 159.9, 152.0, 150.9, 148.2, 145.9, 133.1, 129.2, 128.9, 128.1, 126.9, 124.3, 121.9, 113.1, 108.3, 106.3, 102.3, 98.9, 97.6, 67.5, 55.1, 54.7, 44.3, 12.7; HRMS (ESI-TOF) m/z [M + H]$^+$ Calcd for $C_{35}H_{40}N_3O_2$ 534.3121, found 534.3115.

3′-N,3′-N,6′-N,6′-N-Tetraethyl-2-(4-fluorophenyl)-2,3-dihydrospiro[isoindole-1,9′-xanthene]-3′,6′-diamine (pF-AnMR). Pink viscous oil. Yield 79 mg (81%): R_f = 0.53 in 90:10 Hex:EtOAc; ^{1}H NMR (400 MHz, $CDCl_3$) δ 7.38 (d, J = 7.5 Hz, 1H), 7.20 (t, J = 7.4 Hz, 1H), 7.13 (t, J = 7.5 Hz, 1H), 6.87 (d, J = 7.6 Hz, 1H), 6.76 (dd, J = 12.9, 4.7 Hz, 2H), 6.64 (dd, J = 8.8, 1.2 Hz, 2H), 6.60−6.48 (m, 2H), 6.47−6.36 (m, 2H), 6.20 (dd, J = 8.8, 1.4 Hz, 2H), 5.02 (s, 2H), 3.30 (q, J = 7.0 Hz, 8H), 1.14 (t, J = 7.5, 6.5 Hz, 12H); ^{13}C NMR

(101 MHz, $CDCl_3$) δ 156.2, 153.8, 152.0, 151.1, 148.2, 141.0, 140.9, 132.7, 128.5, 128.1, 126.8, 124.1, 121.9, 115.2, 115.0, 113.83, 113.76, 113.0, 108.0, 97.8, 67.6, 55.4, 44.3, 12.7; HRMS (ESI-TOF) m/z [M + H]$^+$ Calcd for $C_{34}H_{37}N_3OF$ 522.2921, found 522.2914.

3′-N,3′-N,6′-N,6′-N-Tetraethyl-2-(3-fluorophenyl)-2,3-dihydrospiro[isoindole-1,9′-xanthene]-3′,6′-diamine (mF-AnMR). Pink viscous oil. Yield 39 mg (41%): R_f = 0.53 in 90:10 Hex:EtOAc; ^{1}H NMR (400 MHz, $CDCl_3$) δ 7.39 (d, J = 7.5 Hz, 1H), 7.21 (t, J = 7.4 Hz, 1H), 7.13 (t, J = 7.5 Hz, 1H), 6.95 (dd, J = 15.7, 7.8 Hz, 1H), 6.87 (d, J = 7.7 Hz, 1H), 6.64 (d, J = 8.7 Hz, 2H), 6.42 (d, J = 2.5 Hz, 2H), 6.41−6.32 (m, 2H), 6.26 (td, J = 8.4, 2.4 Hz, 1H), 6.21 (dd, J = 8.8, 2.5 Hz, 2H), 5.02 (s, 2H), 3.30 (q, J = 7.0 Hz, 8H), 1.14 (t, J = 7.0 Hz, 12H); ^{13}C NMR (101 MHz, $CDCl_3$) δ 164.7, 162.3, 151.9, 150.9, 148.3, 146.3, 146.2, 132.3, 129.5, 129.4, 128.4, 128.2, 126.9, 124.1, 121.9, 112.7, 109.4, 109.3, 108.1, 102.5, 102.3, 100.7, 100.4, 97.9, 67.8, 55.3, 44.3, 12.7; HRMS (ESI-TOF) m/z [M + H]$^+$ Calcd for $C_{34}H_{37}N_3OF$ 522.2921, found 522.2926.

3′-N,3′-N,6′-N,6′-N-Tetraethyl-2-(4-chlorophenyl)-2,3-dihydrospiro[isoindole-1,9′-xanthene]-3′,6′-diamine (pCl-AnMR). Pink viscous oil. Yield 54 mg (55%): R_f = 0.53 in 90:10 Hex:EtOAc; ^{1}H NMR (400 MHz, $CDCl_3$) δ 7.38 (d, J = 7.3 Hz, 1H), 7.20 (t, J = 7.4 Hz, 1H), 7.13 (t, J = 7.5 Hz, 1H), 6.98 (d, J = 9.0 Hz, 2H), 6.86 (d, J = 7.6 Hz, 1H), 6.61 (d, J = 8.8 Hz, 2H), 6.54 (d, J = 9.0 Hz, 2H), 6.40 (d, J = 2.2 Hz, 2H), 6.19 (dd, J = 8.8, 2.3 Hz, 2H), 5.01 (s, 2H), 3.30 (q, J = 7.0 Hz, 8H), 1.14 (t, J = 7.0 Hz, 12H); ^{13}C NMR (101 MHz, $CDCl_3$) δ 151.9, 150.9, 148.2, 143.0, 132.4, 128.43, 128.41, 128.2, 126.9, 124.1, 121.9, 120.9, 114.4, 112.7, 108.1, 97.8, 67.6, 55.1, 44.3, 12.7; HRMS (ESI-TOF) m/z [M + H]$^+$ Calcd for $C_{34}H_{37}N_3OCl$ 538.2625, found 538.2618.

3′-N,3′-N,6′-N,6′-N-Tetraethyl-2-(3-chlorophenyl)-2,3-dihydrospiro[isoindole-1,9′-xanthene]-3′,6′-diamine (mCl-AnMR). Pink viscous oil. Yield 49 mg (51%): R_f = 0.53 in 90:10 Hex:EtOAc; ^{1}H NMR (400 MHz, $CDCl_3$) δ 7.39 (d, J = 7.5 Hz, 1H), 7.22 (t, J = 7.4 Hz, 1H), 7.14 (t, J = 7.5 Hz, 1H), 6.86 (dd, J = 9.6, 8.5 Hz, 2H), 6.70 (d, J = 2.0 Hz, 1H), 6.63 (d, J = 8.8 Hz, 2H), 6.58−6.49 (m, 1H), 6.48−6.38 (m, 3H), 6.21 (dd, J = 8.8, 2.5 Hz, 2H), 5.02 (s, 2H), 3.31 (q, J = 7.0 Hz, 8H), 1.14 (t, J = 7.0 Hz, 12H); ^{13}C NMR (101 MHz, $CDCl_3$) δ 152.0, 150.8, 148.3, 145.7, 134.3, 132.3, 129.4, 128.5, 128.2, 127.0, 124.2, 121.9, 115.8, 113.1, 112.6, 112.0, 108.2, 97.9, 67.8, 55.1, 44.3, 12.7; HRMS (ESI-TOF) m/z [M + H]$^+$ Calcd for $C_{34}H_{37}N_3OCl$ 538.2625, found 538.2618.

3′-N,3′-N,6′-N,6′-N-Tetraethyl-2-[4-(trifluoromethyl)phenyl]-2,3-dihydrospiro[isoindole-1,9′-xanthene]-3′,6′-diamine (pCF$_3$-AnMR). Pink viscous oil. Yield 89 mg (91%): R_f = 0.51 in 90:10 Hex:EtOAc; ^{1}H NMR (400 MHz, $CDCl_3$) δ 7.40 (d, J = 7.5 Hz, 1H), 7.27 (d, J = 9.4 Hz, 3H), 7.24−7.19 (m, 1H), 7.14 (t, J = 7.4 Hz, 1H), 6.87 (d, J = 7.6 Hz, 1H), 6.66 (d, J = 8.7 Hz, 2H), 6.61 (d, J = 8.8 Hz, 2H), 6.41 (d, J = 2.5 Hz, 2H), 6.20 (dd, J = 8.8, 2.6 Hz, 2H), 5.07 (s, 2H), 3.30 (q, J = 7.1 Hz, 8H), 1.14 (t, J = 7.0 Hz, 12H); ^{13}C NMR (101 MHz, $CDCl_3$) δ 151.9, 150.6, 148.3, 146.8, 132.1, 128.4, 127.1, 125.9 (q, J^3 = 3.8 Hz), 125.2 (q, J^1 = 269 Hz), 124.2, 121.9, 117.3 (q, J^2 = 32.4 Hz), 112.8, 112.3, 108.1, 97.8, 67.9, 55.1, 44.3, 12.7; HRMS (ESI-TOF) m/z [M + H]$^+$ Calcd for $C_{35}H_{37}N_3OF_3$ 572.2889, found 572.2882.

3′-N,3′-N,6′-N,6′-N-Tetraethyl-2-[3-(trifluoromethyl)phenyl]-2,3-dihydrospiro[isoindole-1,9′-xanthene]-3′,6′-diamine (mCF$_3$-AnMR). Pink viscous oil. Yield 92 mg (94%): R_f = 0.54 in 90:10 Hex:EtOAc; ^{1}H NMR (400 MHz, $CDCl_3$) δ 7.41 (d, J = 7.5 Hz, 1H), 7.23 (td, J = 7.4, 1.2 Hz, 1H), 7.18−7.11 (m, 1H), 7.01 (t, J = 8.0 Hz, 1H), 6.91 (t, J = 2.1 Hz, 1H), 6.87 (d, J = 7.6 Hz, 1H), 6.79 (d, J = 7.3 Hz, 1H), 6.67 (dd, J = 8.5, 2.6 Hz, 1H), 6.61 (d, J = 8.8 Hz, 2H), 6.41 (d, J = 2.5 Hz, 2H), 6.20 (dd, J = 8.8, 2.6 Hz, 2H), 5.05 (s, 2H), 3.29 (q, J = 7.1 Hz, 8H), 1.13 (t, J = 7.0 Hz, 12H); ^{13}C NMR (101 MHz, $CDCl_3$) δ 152.0, 150.6, 148.3, 144.6, 132.4, 130.6, 128.7, 128.5, 128.2, 127.0, 124.2, 121.9, 116.5, 112.3, 112.3, 109.3, 109.3, 108.2, 97.8, 67.7 55.0, 44.3, 12.6; HRMS (ESI-TOF) m/z [M + H]$^+$ Calcd for $C_{35}H_{37}N_3OF_3$ 572.2889, found 572.2896.

Synthesis of the AnMR6G Series. Compound **13** was synthesized according to the literature.[22]

A general procedure for preparing the rhodamine 6G amides (**14**−**17**) was used. To a solution of **13** (200 mg, 0.44 mmol) in 1,2-dichloroethane (10 mL) was added phosphorus oxychloride (0.3 mL, 3 mmol) dropwise. The solution was refluxed for 4 h. The reaction mixture was cooled and evaporated under reduced pressure to give the rhodamine 6G acid chloride, which was used in the next step without further purification. To the crude acid chloride dissolved in 1,2-dichloroethane (10 mL) was added 0.1 mL of the corresponding aniline. The mixture was added to a separatory funnel with an additional 20 mL of DCM. The organic layer was washed with 2.0 M H_2SO_4 (3 × 20 mL), and then with water (2 × 20 mL), and finally 0.10 M NaOH (2 × 20 mL). The organic layer was then dried over anhydrous $MgSO_4$ and the volatiles were removed under reduced pressure. The products were purified by column chromatography on alumina (neutral) with 70:30 hexanes:EtOAc.

*3′,6′-Bis(ethylamino)-2′,7′-dimethyl-2-phenyl-2,3-dihydrospiro-[isoindole-1,9′-xanthene]-3-one (**14**).* Pink amorphous solid. Yield 180 mg (83%): R_f = 0.23 in 70:30 Hex:EtOAc; ^{1}H NMR (400 MHz, $CDCl_3$) δ 8.15−7.94 (m, 1H), 7.50 (dd, J = 5.7, 3.1 Hz, 2H), 7.18−6.98 (m, 4H), 6.76 (dd, J = 7.9, 1.9 Hz, 2H), 6.44 (s, 2H), 6.23 (s, 2H), 3.48 (s, 4H), 1.94 (s, 6H), 1.30 (t, J = 7.1 Hz, 6H); ^{13}C NMR (101 MHz, $CDCl_3$) δ 167.7, 153.3, 151.5, 147.2, 136.6, 132.9, 131.0, 128.5, 128.1, 127.1, 126.6, 124.0, 123.4, 117.9, 106.9, 105.0, 96.6, 67.5, 38.4, 29.7, 28.0, 16.8, 14.7; HRMS (ESI-TOF) m/z [M + H]$^+$ Calcd for $C_{32}H_{32}N_3O_2$ 490.2495, found 490.2498.

*3′,6′-Bis(ethylamino)-2-(4-methoxyphenyl)-2′,7′-dimethyl-2,3-dihydrospiro[isoindole-1,9′-xanthene]-3-one (**15**).* Pink amorphous solid. Yield 150 mg (65%): R_f = 0.13 in 70:30 Hex:EtOAc; ^{1}H NMR (400 MHz, $CDCl_3$) δ 8.18−7.95 (dd, J = 5.9, 2.8 Hz, 1H), 7.60−7.40 (m, 2H), 7.17−7.06 (dd, J = 5.8, 2.8 Hz, 1H), 6.67−6.51 (m, 4H), 6.43 (s, 2H), 6.22 (s, 2H), 3.67 (s, 3H), 3.56−3.28 (S, 2H), 3.16 (q, J = 7.1 Hz, 4H), 1.95 (s, 6H), 1.30 (t, J = 7.1 Hz, 6H). 13C NMR (101 MHz, $CDCl_3$) δ 151.4, 150.6, 150.3, 146.5, 139.1, 133.1, 128.8, 128.0, 126.7, 124.1, 121.8, 117.5, 114.3, 114.3, 114.1, 114.0, 113.9, 96.6, 67.4, 55.6, 55.3, 38.5, 17.0, 14.9; HRMS (ESI-TOF) m/z [M + H]$^+$ Calcd for $C_{33}H_{34}N_3O_3$ 520.2600, found 520.2600.

*2-(4-Chlorophenyl)-3′,6′-bis(ethylamino)-2′,7′-dimethyl-2,3-dihydrospiro[isoindole-1,9′-xanthene]-3-one (**16**).* Pink amorphous solid. Yield 161 mg (70%): R_f = 0.39 in 70:30 Hex:EtOAc; ^{1}H NMR (400 MHz, $CDCl_3$) δ 8.01 (d, J = 3.4 Hz, 1H), 7.66−7.37 (m, 2H), 7.22−6.94 (m, 3H), 6.73 (d, J = 8.7 Hz, 2H), 6.39 (s, 2H), 6.24 (s, 2H), 3.49 (s, 2H), 3.17 (q, J = 7.0 Hz, 1H), 1.93 (s, 6H), 1.31 (t, J = 7.1 Hz, 6H); ^{13}C NMR (101 MHz, $CDCl_3$) δ 167.7, 153.3, 151.5, 147.4, 135.3, 133.1, 132.1, 130.6, 128.7, 128.3, 128.3, 128.1, 124.0, 123.3, 118.0, 106.4, 105.0, 96.6, 67.6, 38.3, 38.2, 16.8, 14.7, 14.7, 14.6; HRMS (ESI-TOF) m/z [M + H]$^+$ Calcd for $C_{32}H_{31}N_3O_2Cl$ 524.2105, found 524.2098.

*3′,6′-Bis(ethylamino)-2′,7′-dimethyl-2-[4-(trifluoromethyl)-phenyl]-2,3-dihydrospiro[isoindole-1,9′-xanthene]-3-one (**17**).* Pink amorphous solid. Yield 180 mg (73%): R_f = 0.48 in 70:30 Hex:EtOAc; ^{1}H NMR (400 MHz, $CDCl_3$) δ 8.07−7.94 (m, 1H), 7.59−7.44 (m, 2H), 7.36 (d, J = 8.5 Hz, 2H), 7.10 (d, J = 8.3 Hz, 3H), 6.41 (s, 2H), 6.27 (s, 2H), 3.50 (s, 2H), 3.25−3.01 (m, 4H), 1.92 (s, 6H), 1.31 (t, J = 7.1 Hz, 6H); ^{13}C NMR (101 MHz, $CDCl_3$) δ 168.1, 153.7, 151.3, 147.5, 140.4, 133.6, 133.4, 129.8, 128.6, 128.3, 128.2, 128.1, 128.0, 127.8, 127.7, 127.4, 125.7, 125.7, 125.6, 125.6, 125.6, 125.5, 125.4, 124.0, 123.9, 123.9, 123.6, 123.5, 123.4, 122.7, 118.2, 106.4, 96.7, 67.6, 38.3, 16.8, 14.6; HRMS (ESI-TOF) m/z [M + H]$^+$ Calcd for $C_{33}H_{31}N_3O_2F_3$ 558.2368, found 558.2366.

A general procedure for AnMR6G, pMeO-AnMR6G, pCl-AnMR6G, and pCF$_3$-AnMR6G was used. In a 50 mL round-bottom flask, 100 mg of the rhodamine amide was dissolved in 30 mL of dry THF. To this solution, 80 mg of $LiAlH_4$ was slowly added, and the mixture was stirred at room temperature for 12 h. Then the reaction was quenched by slowly adding 0.5 mL of water, followed by 1 mL of 15% NaOH. The mixture was filtered, and the filtrate was dried using $MgSO_4$. The volatiles were removed under reduced pressure. The products were purified by column chromatography on alumina (neutral) with 90:10 hexanes:EtOAc.

3′-N,6′-N-Diethyl-2′,7′-dimethyl-2-phenyl-2,3-dihydrospiro-[isoindole-1,9′-xanthene]-3′,6′-diamine (AnMR6G). Pink amorphous solid. Yield 54 mg (56%): R_f = 0.32 in 90:10 Hex:EtOAc; ^{1}H NMR

dx.doi.org/10.1021/jo401323g | J. Org. Chem. 2013, 78, 10134−10143

(400 MHz, $CDCl_3$) δ 7.43 (d, J = 7.5 Hz, 1H), 7.23 (t, J = 7.4 Hz, 1H), 7.13 (t, J = 7.5 Hz, 1H), 7.05 (t, J = 7.8 Hz, 2H), 6.84 (d, J = 7.7 Hz, 1H), 6.66 (d, J = 8.1 Hz, 2H), 6.57 (t, J = 7.0 Hz, 1H), 6.46 (s, 2H), 6.40 (s, 2H), 5.08 (s, 2H), 3.34 (s, 2H), 3.21 (q, J = 7.2 Hz, 4H), 1.84 (s, 6H), 1.31 (t, J = 7.1 Hz, 6H); ^{13}C NMR (101 MHz, $CDCl_3$) δ 151.2, 150.2, 146.5, 144.5, 132.7, 128.7, 128.6, 128.5, 128.1, 126.7, 124.2, 121.8, 117.5, 115.7, 113.6, 113.5, 113.4, 96.6, 67.5, 55.0, 38.5, 17.0, 14.7; HRMS (ESI-TOF) m/z $[M + H]^+$ Calcd for $C_{32}H_{34}N_3O$ 476.2702, found 476.2702.

3′-N,6′-N-Diethyl-2-(4-methoxyphenyl)-2′,7′-dimethyl-2,3-dihydrospiro[isoindole-1,9′-xanthene]-3′,6′-diamine (pMeO-AnMR6G). Pink amorphous solid. Yield 88 mg (90%): R_f = 0.19 in 90:10 Hex:EtOAc; ^{1}H NMR (400 MHz, $CDCl_3$) δ 7.40 (d, J = 7.5 Hz, 1H), 7.21 (t, J = 6.9 Hz, 1H), 7.11 (t, J = 7.5 Hz, 1H), 6.85−6.76 (m, 1H), 6.64 (d, J = 9.2 Hz, 2H), 6.56 (d, J = 9.3 Hz, 2H), 6.44 (s, 2H), 6.37 (s, 2H), 5.02 (s, 2H), 3.64 (s, 3H), 3.33 (s, 2H), 3.19 (q, J = 7.1 Hz, 4H), 1.84 (s, 6H), 1.30 (t, J = 7.1 Hz, 6H); ^{13}C NMR (101 MHz, $CDCl_3$) δ 167.7, 158.2, 153.1, 151.7, 147.2, 132.7, 131.4, 129.0, 128.9, 128.6, 128.1, 124.1, 123.3, 117.8, 113.9, 106.8, 96.6, 67.5, 55.11, 38.4, 16.8, 14.7; HRMS (ESI-TOF) m/z $[M + H]^+$ Calcd for $C_{33}H_{36}N_3O_2$ 506.2808, found 506.2805.

2-(4-Chlorophenyl)-3′-N,6′-N-diethyl-2′,7′-dimethyl-2,3-dihydrospiro[isoindole-1,9′-xanthene]-3′,6′-diamine (pCl-AnMR6G). Pink amorphous solid. Yield 75 mg (77%): R_f = 0.32 in 90:10 Hex:EtOAc; ^{1}H NMR (400 MHz, $CDCl_3$) δ 7.40 (d, J = 7.5 Hz, 1H), 7.22 (t, J = 7.4 Hz, 1H), 7.12 (t, J = 7.5 Hz, 1H), 6.95 (d, J = 8.7 Hz, 2H), 6.81 (d, J = 7.7 Hz, 1H), 6.53 (d, J = 8.9 Hz, 2H), 6.39 (s, 2H), 6.36 (s, 2H), 5.01 (s, 2H), 3.35 (s, 2H), 3.19 (q, J = 7.2 Hz, 4H), 1.84 (s, 6H), 1.30 (t, J = 7.1 Hz, 6H); ^{13}C NMR (101 MHz, $CDCl_3$) δ 150.9, 150.2, 146.7, 143.1, 132.5, 128.5, 128.4, 128.2, 126.8, 124.2, 121.8, 120.8, 117.6, 114.3, 113.1, 96.6, 67.7, 55.1, 38.4, 17.0, 14.8; HRMS (ESI-TOF) m/z $[M + H]^+$ Calcd for $C_{32}H_{33}N_3OCl$ 510.2312, found 510.2319.

3′-N,6′-N-Diethyl-2′,7′-dimethyl-2-[4-(trifluoromethyl)phenyl]-2,3-dihydrospiro[isoindole-1,9′-xanthene]-3′,6′-diamine (pCF$_3$-AnMR6G). Pink amorphous solid. Yield 71 mg (73%): R_f = 0.30 in 90:10 Hex:EtOAc; ^{1}H NMR (400 MHz, $CDCl_3$) δ 7.42 (d, J = 7.5 Hz, 1H), 7.25 (m, 3H), 7.14 (t, J = 7.5 Hz, 1H), 6.82 (d, J = 7.7 Hz, 1H), 6.65 (d, J = 8.5 Hz, 2H), 6.37 (s, 4H), 5.07 (s, 2H), 3.37 (s, 2H), 3.20 (q, J = 7.2 Hz, 4H), 1.84 (s, 6H), 1.31 (t, J = 7.1 Hz, 6H); ^{13}C NMR (101 MHz, $CDCl_3$) δ 150.7, 150.2, 146.9, 146.8, 132.1, 128.5, 128.4, 127.0, 125.8, 125.8, 125.7, 124.3, 121.9, 117.7, 112.8, 112.7, 112.6, 96.6, 68.0, 55.1, 38.4, 17.0, 14.8; HRMS (ESI-TOF) m/z $[M + H]^+$ Calcd for $C_{33}H_{33}N_3OF_3$ 544.2576, found 544.2582.

Synthesis of AMR and AMR6G.

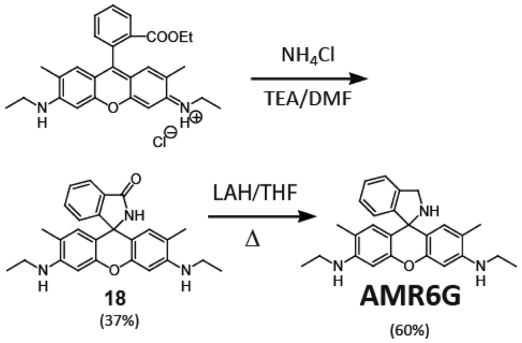

AMR was synthesized according to procedures in the literature.[14]

*3′,6′-Bis(ethylamino)-2′,7′-dimethyl-2,3-dihydrospiro[isoindole-1,9′-xanthene]-3-one (**18**).* In a 250 mL Erlenmeyer flask, 10 g of NH_4Cl was added to a mixture of DMF (25 mL) and TEA (25 mL). The flask was capped and the mixture was allowed to stir for two hours before adding 1 g (2.1 mmol) of rhodamine 6G. This mixture was then stirred for an additional 48 h. The product was isolated by pouring the reaction mixture in 125 mL of ice/cold water and then transferring to a separatory funnel. The product was extracted from the aqueous mixture using DCM (3 × 25 mL). The combined organic layers were dried using Na_2SO_4, and the solvent was removed in vacuo. The crude oil was purified by column chromatography using 70/30 (Hex/EtOAc) yielding 310 mg (37%) of **2**−**9** as a white solid that turned pink soon after: ^{1}H NMR (400 MHz, $CDCl_3$) δ 7.89 (dd, J = 5.6, 3.2 Hz, 1H), 7.42 (dd, J = 5.7, 3.1 Hz, 2H), 7.00 (dd, J = 5.7, 3.0 Hz, 1H), 6.54 (s, 2H), 6.42 (s, 1H), 6.35 (s, 2H), 3.49 (s, 2H), 3.21 (q, J = 7.1 Hz, 4H), 1.94 (s, 6H), 1.32 (t, J = 7.1 Hz, 6H); ^{13}C NMR (101 MHz, $CDCl_3$) δ 169.9, 155.8, 150.7, 147.2, 132.9, 129.4, 128.0 (d, J = 15.1 Hz), 123.6, 123.2, 117.8, 107.7, 96.7, 76.7, 60.0, 38.4, 16.7, 14.7; HRMS (ESI-TOF) m/z $[M + H]^+$ Calcd for $C_{26}H_{28}N_3O_2$ 414.2182, found 414.2178

3′-N,6′-N-Diethyl-2′,7′-dimethyl-2,3-dihydrospiro[isoindole-1,9′-xanthene]-3′,6′-diamine (AMR6G). In a 100 mL round-bottom flask, 200 mg of **2**−**9** was dissolved in 50 mL of dry THF. To this solution, 180 mg of LAH was added slowly. The solution was then refluxed under argon for 48 h. The reaction mixture was cooled using an ice bath and then quenched using 0.5 mL water and 1.5 mL of 10% NaOH solution. The mixture was filtered and the filtrate dried with $MgSO_4$ followed by removal of the volatiles under reduced pressure. The crude was purified by column chromatography to give 116 mg (60%) of AMR6G as a pink amorphous solid: ^{1}H NMR (400 MHz, $CDCl_3$) δ 7.42−7.05 (m, 3H), 6.90 (d, J = 7.6 Hz, 1H), 6.57 (s, 2H), 6.49 (s, 1H), 6.33 (s, 2H), 4.50 (s, 2H), 3.39 (s, 2H), 3.20 (q, J = 6.7 Hz, 4H), 1.96 (s, 6H), 1.30 (t, J = 7.1 Hz, 6H); ^{13}C NMR (101 MHz, $CDCl_3$) δ 149.9, 148.6, 146.4, 146.0, 140.3, 131.3, 130.5, 130.3, 129.2, 127.7, 127.1−126.8 (m), 124.9, 122.0, 117.4, 116.8, 115.8, 111.9, 97.4, 96.6, 77.4, 65.7, 51.3, 43.6, 38.5 (d, J = 4.3 Hz), 17.0, 16.8, 14.9 (d, J = 3.5 Hz); HRMS (ESI-TOF) m/z $[M + H]^+$ Calcd for $C_{26}H_{28}N_3O_2$ 414.2182, found 414.2178.

■ ASSOCIATED CONTENT

Supporting Information

UV−vis and fluorescence pH titration curves, quantum yield studies, analogue structures, NMR experiments, and NMR spectra. These materials are available free of charge via the Internet at http://pubs.acs.org.

■ AUTHOR INFORMATION

Corresponding Author

*E-mail: cscott@chem.siu.edu.

Notes

The authors declare no competing financial interest.

■ ACKNOWLEDGMENTS

The authors gratefully acknowledge support fully or in part from the National Institutes of Health (NIH-1R15GM080721-01A1) and the National Science Foundation (NSF-CHEM-0719185). The authors also thank the Department of Chemistry and Biochemistry, Southern Illinois University, for partial support of this research.

■ REFERENCES

(1) Ohkuma, S.; Poole, B. *Proc. Natl. Acad. Sci. U. S. A.* **1978**, *75*, 3327.

(2) Paroutis, P.; Touret, N.; Grinstein, S. *Physiology* **2004**, *19*, 207.

(3) Holopainen, J. M.; Saarikoski, J.; Kinnunen, P. K. J.; Jarvela, I. *Eur. J. Biochem.* **2001**, *268*, 5851.

(4) Smith, J. L. J. *Food Proteins* **2003**, *66*, 1292−1303. (b) Giannella, R. A.; Broitman, S. A.; Zamcheck, N. *Gut* **1972**, *13*, 251−256.

(5) Martinsen, T. C.; Bergh, K.; Waldum, H. L. *Basic Clin. Pharmacol. Toxicol.* **2005**, *96*, 94−102.

(6) (a) Papavramidis, T. S.; Papavramidis, S. T.; Sapalidis, K. G.; Kessisoglou, I. I.; Gamvros, O. I. *Obes. Surg.* **2004**, *14*, 271−274. (b) Huang, J. Q.; Hunta, R. H. *Yale J. Biol. Med.* **1996**, *69*, 159−174.

(7) Vavere, A. L.; Biddlecombe, G. B.; Spees, W. M. *Cancer Res.* **2009**, *69*, 4510.

(8) Gallagher, F. A.; Kettunen, M. I.; Day, S. E. *Nature* **2008**, *453*, 940.

(9) Han, J.; Burgess, K. *Chem. Rev.* **2010**, *110*, 2709.
(10) (a) Lin, H.-J.; Szmacinski, H.; Lakowicz, J. R. *Anal. Biochem.* **1999**, *269*, 162. (b) Nedergaard, M.; Desai, S.; Pulsinelli, W. *Anal. Biochem.* **1990**, *187*, 109.
(11) (a) Myochin, T.; Kiyose, K.; Hanaoka, K.; Kojima, H.; Terai, T.; Nagano, T. *J. Am. Chem. Soc.* **2011**, *133*, 3401. (b) Kiyose, K.; Aizawa, S.; Sasaki, E.; Kojima, H.; Hanaoka, K.; Terai, T.; Urano, Y.; Nagano, T. *Chem.—Eur. J.* **2009**, *15*, 9191.
(12) Chen, X.; Pradhan, T.; Wang, F.; Kim, J. S.; Yoon, J. *Chem. Rev.* **2012**, *112*, 1910.
(13) (a) Li, Z.; Song, Y.; Yang, Y.; Yang, L.; Huang, X.; Han, J.; Han, S. *Chem. Sci.* **2012**, *3*, 2941. (b) Montenegro, H.; Di Paolo, M.; Capdevila, D.; Aramendía, P. F.; Bossi, M. L. *Photochem. Photobiol. Sci.* **2012**, *11*, 1081. (c) Tian, M.; Peng, X.; Fan, J.; Wang, J.; Sun, S. *Dyes Pigm.* **2012**, *95*, 112. (d) Hu, Z.; Li, M.; Liu, M.; Zhuang, W.; Li, G. *Dyes Pigm.* **2013**, *96*, 71. (e) Lv, H.; Liu, J.; Zhao, J.; Zhao, B.; Miao, J. *Sens. Actuators, B* **2013**, *177*, 956.
(14) Best, Q. A.; Xu, R.; McCarroll, M. E.; Wang, L.; Dyer, D. J. *Org. Lett.* **2010**, *12*, 3219.
(15) Wu, Z.; Wu, X.; Yang, Y.; Wen, T.; Han, S. *Bioorg. Med. Chem. Lett.* **2012**, *22*, 6358.
(16) Wu, X.; Wu, Z.; Yang, Y.; Han, S. *Chem. Commun.* **2012**, *48*, 1895.
(17) Li, Z.; Xue, Z.; Wu, Z.; Han, J.; Han, S. *Org. Biomol. Chem.* **2011**, *9*, 7652.
(18) Bender, A.; Woydziak, Z. R.; Fu, L.; Branden, M.; Zhou, Z.; Ackley, B. D.; Peterson, B. R. *ACS Chem. Bio.* **2013**, *8*, 636−642.
(19) Kubin, R. F.; Fletcher, A. N. *J. Lumin.* **1982**, *27*, 455−462.
(20) Casey, K. G.; Quitevis, E. L. *J. Phys. Chem.* **1988**, *92*, 6590−6594.
(21) Gross, K. C.; Seybold, P. G. *Int. J. Quantum Chem.* **2000**, *80*, 1107.
(22) Li, H.; Fan, J.; Wang, J.; Tian, M.; Du, J.; Sun, S.; Sun, P.; Peng, X. *Chem. Commun.* **2009**, *45*, 5904.